High-temperature oxidation behavior of aluminized AISI 4130 steel

By Muhammad Badaruddin

High-temperature oxidation behavior of aluminized AISI 4130 steel

Mohammad Badaruddin, Chaur Jeng Wang, Herry Wardono, Tarkono, and Dwi Asmi

Citation: AIP Conference Proceedings **1711**, 040002 (2016); doi: 10.1063/1.4941624
View online: http://dx.doi.org/10.1063/1.4941624
View Table of Contents: http://scitation.aip.org/content/aip/proceeding/aipcp/1711?ver=pdfcov
Published by the AIP Publishing

High-Temperature Oxidation Behavior of Aluminized AISI 4130 Steel

Mohammad Badaruddin[1,a)], Chaur Jeng Wang[3)], Herry Wardono[1)], Tarkono[1)], and Dwi Asmi[2)]

[1]*Mechanical Engineering Department, Engineering Faculty, Lampung University*
[2]*Physics Department, Mathematics and Natural Sciences Faculty, Lampung University*
Jalan Soemantri Brojonegoro No.1, Bandar Lampung 35145, Indonesia
[3]*Mechanical Engineering Department, National Taiwan University of Science and Technology (NTUST)*
43 Keelung Rd, Sec. 4, Taipei 106, Taiwan, ROC

[a]Corresponding author: mbruddin@eng.unila.ac.id

Abstract. AISI 4130 steel was dipped into a molten aluminum bath at 700°C for 16 s to produce an aluminide coating on the steel substrate. The coating, which consisted of an Al-rich layer and an $FeAl_3$ and Fe_2Al_5 intermetallic layer, strongly adhered to the steel substrate. High-temperature oxidation of the bare steel and aluminized steel was performed by thermogravimetry at 850°C for 49 h in static air. The oxidation products were characterized by scanning electron microscopy and energy-dispersive spectroscopy. The aluminide coating could increase the oxidation resistance of the bare steel by a factor of ~19. The increase in high-temperature oxidation resistance of the aluminized steel is attributed to the formation of protective alumina scale (α-Al_2O_3). Although iron oxide nodules grew on the aluminide coating surface, the oxidation rate of the aluminide coatings was very low. After 49 h of oxidation, agglomerates of α-Al_2O_3 fine grains grew on the rod-shaped FeAl phases.

INTRODUCTION

AISI 4130 steel containing 1.10 wt.%Cr and 0.25 wt.%Mo may be a candidate material for structural engineering components. Cr–Mo steel alloys have been widely used as engineering components in power plants, incinerators, and in the petrochemical industry as boilers or heat exchangers for use at a working temperature of ~550°C [1,2]. However, chromia scale (Cr_2O_3) formed on Cr–Mo steel alloys used at high working temperatures degrades rapidly because of the formation of nonprotective iron oxide (Fe_2O_3) scale [3]. Consequently, the engineering components are severely damaged under service conditions.

One technique for improving the oxidation resistance of steel at high temperatures is the use of hot-dipped aluminum coating. Studies on the oxidation behavior of hot-dipped aluminide steel have revealed that the steel after hot-dipped aluminum coating possesses higher isothermal oxidation resistance compared with that of steel with a chromia former [4,5]. The aluminide coating can protect the steel substrate from aggressive attack by oxidizing or corrosive gas in the environment by forming of a highly protective Al_2O_3 layer during exposure to high temperatures [5–9]. Therefore, it is necessary to investigate the high-temperature oxidation behavior of hot-dipped aluminum coatings on AISI 4130 steel. Therefore, we attempted in the present study to isothermally oxidize hot-dipped aluminide AISI 4130 steel at 850°C for 49 h. The high-temperature oxidation behavior of the resulting steel with aluminized coating was studied by examining the oxidation kinetics, as well as the changes in microstructure and surface morphology of the aluminide coating.

International Symposium on Frontier of Applied Physics (ISFAP) 2015
AIP Conf. Proc. 1711, 040002-1–040002-6; doi: 10.1063/1.4941624

EXPERIMENTAL PROCEDURE

The substrates were cut into specimens with dimensions of 20 mm × 10 mm × 2 mm from commercial AISI 4130 steel. Before the aluminizing coating procedure, all specimens were ultrasonically etched with a solution of 5% NaOH for 30 s and then with 10% H_3PO_4 for 15 s. After the etching step, specimens were washed with water at a temperature of <30°C. Immediately after washing, the etched specimens were subjected to uniform flux application using a welding Al flux. Each specimen was then dipped into a bath of molten 99.0 wt.%Al at 700°C. The specimens were moved at the appropriate speed by a hook made of stainless-steel wire to a crane system. After each specimen was immersed for 16 s, it was removed from the molten Al bath and then cooled in air at room temperature. The oxide flux thus formed on the surface of the aluminized specimen was then cleaned by using a nitric acid/phosphoric acid/water solution (1:1:1 v/v) at room temperature.

The oxidation kinetics of the uncoated and Al-coated specimens was separately studied by thermogravimetric analysis in ambient air at 850°C for at various times within 49 h. In order to investigate the oxidation behavior of aluminized AISI 4130 steel, Al-coated steel specimens were oxidized in a box furnace at 850°C at various times within 49 h and then air-cooled. The oxidation kinetics was monitored by plotting data for the weight gain (mg cm^{-2}) versus square root of time ($s^{1/2}$) curve. Samples were characterized by identifying structures of scale and phase formed by X-ray diffraction analysis in Bragg–Brentano configuration using monochromatic Cu-Kα radiation at 40 kV and 100 mA. Furthermore, the surface morphology, cross sections, and element compositions (at.%) of the specimens were examined by scanning electron microscopy (SEM) using secondary electron image signals and energy-dispersive spectroscopy (EDS).

RESULTS AND DISCUSSION

Performance during High-Temperature Oxidation

A plot of the weight gain versus square root of time is displayed in Fig. 1. The oxidation resistance of the Al-coated specimen markedly increased at 850°C for 49 h because the protective Al-rich oxide layer (Al_2O_3) that formed protected the steel from high-temperature oxidation. After 49 h of exposure to 850°C, the weight gain of the Al-coated steel and the bare steel was about 1.218 and 23.309 mg cm^{-2}, respectively. According to linear regression results (Fig. 1), the parabolic rate constant (k_p) of bare steel is around 5.43×10^{-9} mg^2 cm^{-4} s^{-1} during oxidation times ranging from 3 to 16 h. If the k_p value of the Al-coated steel is compared with the k_p value of bare steel, then the k_p value for the Al-coated steel is two to four orders of magnitude lower than that for bare steel. The k_p value for aluminized AISI 4130 steel in the present study is one to two orders of magnitude higher than those of Fe–Cr alloys with Al coating in other studies [4,5].

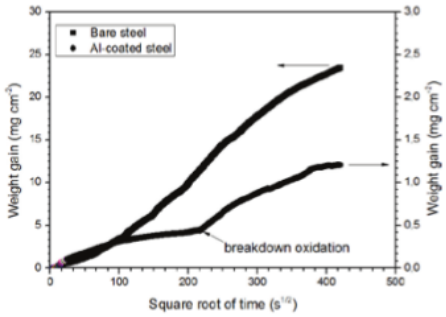

FIGURE 1. Weight gain versus square root of time for bare steel and for aluminized AISI 4130 steel after oxidation at 850°C for 49 h

As can be seen in Fig. 1, the oxidation kinetics of Al-coated steel during the 4 h oxidation period follows a parabolic trend, having a k_p value of 6.74×10^{-12} mg^2 cm^{-4} s^{-1}. After >4 h of exposure, the oxidation rate of Al-coated steel steadily decreased that was indicated by a decrease in k_p value to 7.17×10^{-13} mg^2 cm^{-4} s^{-1}. Furthermore, the weight gain of Al-coated steel increased rapidly as the oxidation time increased to 15 h (Fig. 1). The k_p value of Al-coated

steel increased by two orders of magnitude (k_p = 1.50 × 10^{-11} mg^2 cm^{-4} s^{-1}) relative to that of oxidation rate of bare steel. Although the surface of the aluminide layer of the Al-coated specimens was dense and compact, iron oxide nodules grew on the surface. Figure 2 shows a SEM micrograph of the surface morphology of the Al-coated steel after isothermal oxidation at 850°C in air. The iron oxide nodules began to grow on the aluminide coating at an oxidation time of 15 h. In this case, iron oxide nodules growing locally on the aluminide layer contributed to an increase in the oxidation rate of Al-coated steel. Similar cases of oxidation of mild steel with a hot-dipped aluminum coating and exposed to 850°C in dry air [6] and to 750°C in a steam environment [7] have been reported.

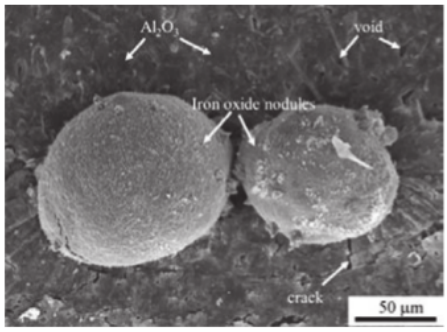

FIGURE 2. Surface morphology of the Al-coated specimen following oxidation at 850°C for 15 h showing the growth of iron oxide nodules

As shown by the SEM micrograph in Fig. 2, iron oxide nodules were found on the aluminide coating layer. However, not all of the nodules were located on the surface of the aluminide coating. Breakdown oxidation in Fig. 1 may be due to sporadic growth of iron oxide nodules. Iron oxide nodules can grow on the surface of the aluminide coating in two ways: (1) Oxygen penetrating the steel substrate via crack paths and steel substrate is oxidized directly by oxygen [6]. (2) Al''' vacancy defects in alumina scale allow outward diffusion of Fe^{2+} through Al_2O_3 via aluminum vacancies; subsequently, iron oxidation mechanism dominates and forms iron oxide nodules [7].

Microstructures Observation and Characterization

The cross-sectional micrograph of the aluminide layer after the aluminizing process is shown in Fig. 3a. The thickness of the aluminide coating is about 24 μm, 18 μm of which consists of $FeAl_3$ and Fe_2Al_5 layers. No cracks or dense structures could be observed in the aluminide layer on the steel substrate. According to EDS analysis, the Al, Fe, Cr compositions (at.%) of $FeAl_3$ and Fe_2Al_5 were 80.11, 19.8, and 0.09 and 69.29, 30.31, and 0.39, respectively. The flat Fe_2Al_5 structure at the interface had a phase containing a low concentration of Cr [8].

In order to understand the high-temperature oxidation behavior of aluminized AISI 4130 steel, the Al-coated steel specimens were isothermally oxidized at 850°C for various durations within 49 h. The SEM micrograph of the cross-sectional Al-coated steel specimen after 1 h of oxidation shows that the Al and $FeAl_3$ layers of the as-coated specimen disappeared and transformed into Fe_2Al_5 and $FeAl_2$ (Fig. 3b). Moreover, FeAl–Cr precipitates with high Cr content could be observed in the Fe_2Al_5 and $FeAl_2$ layers. These precipitates were generated by rapid dilution of the Fe-rich region due to diffusion coupling between internal Al atoms and external Fe atoms. Al, Fe, and Cr, compositions (at.%) of the FeAl–Cr precipitate were 41.19, 55.38, and 3.43, respectively. No molybdenum could detected by EDS analysis. Some voids that formed and dispersed in the outer aluminide layer can also be observed in Fig. 3b. Phase transformation during oxidation at high temperatures induced by the volume change of intermetallic phases contributed to void formation [9].

It also can be observed in Fig. 3c and 3d that the $Fe_2Al_5/FeAl_2$ layer dominantly formed in the aluminide layer, whereas a thin FeAl layer formed on the steel substrate. The result for EDS oxygen mapping (Fig. 3e) indicates that a very thin Al_2O_3 layer formed in the outer aluminide layer with Fe atoms dissolved in the alumina scale after an oxidation time of 1 h. Some voids that formed in the outer aluminide layer show that aluminum atoms in the Fe_2Al_5 phase diffused outward and subsequently contributed to Al_2O_3 formation (Fig. 3e). EDS analysis of the spectrum of the aluminide layer showed that the Cr composition was around 0.43 to 1.72 at.% (Fig. 3f).

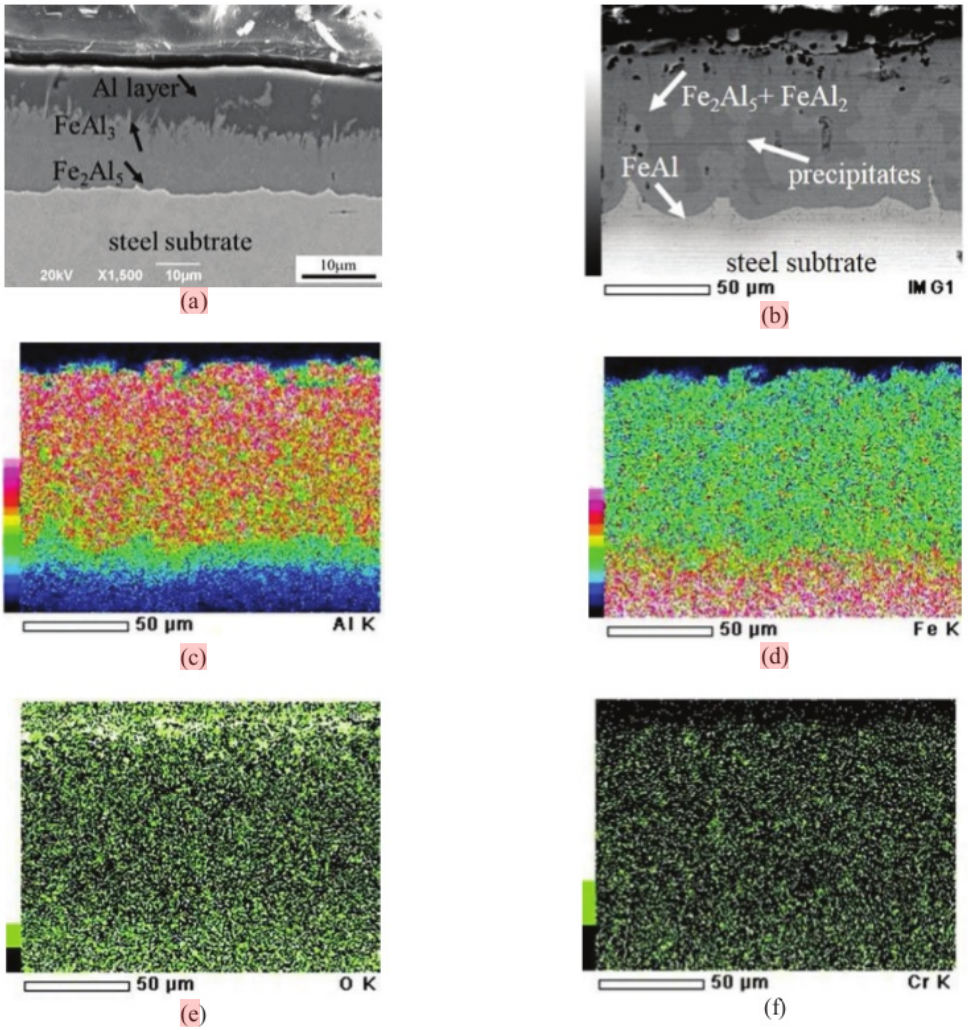

FIGURE 3. SEM micrographs of (a) the as-coated steel and of (b) the Al-coated specimen oxidized for 1 h. (c–f) EDS elemental maps for Al, Fe, O and Cr in the specimen in part b

Phase transformation and microstructure evolution behaviors of the aluminide layer on the hot-dipped aluminized Cr–Mo steel after isothermal oxidation for shorter time were examined. Fe_2Al_5, $FeAl_2$, and FeAl were precipitates with high Cr content in the FeAl–Cr phase in the aluminide coating [9]. As the oxidation time increased to 36 h, aluminum atoms diffused rapidly into the steel substrate, resulting in a decrease in their concentration. The Fe_2Al_5 phase was replaced by $FeAl_2$ and FeAl phases via interdiffusion between internal Al atoms and external Fe atoms from the substrate. The SEM cross-sectional micrograph of the Al-coated specimen oxidized at 850°C for 36 h and its corresponding EDS line profiles of Fe, Al, O, Cr, and Mo distributions across the coating layer on the steel substrate are depicted in Fig. 4. The two distinct phases in the aluminide layer consisted of FeAl, $FeAl_2$, and a thin Al_2O_3 scale. The composition of iron atoms in the Al_2O_3 scale ranged from 9.1 to 11.3 at.%, and that of Cr atoms was only ~0.66 at.%. Both Fe and Cr are well-known metals that support rapid formation of very stable α-Al_2O_3 [2,4,10].

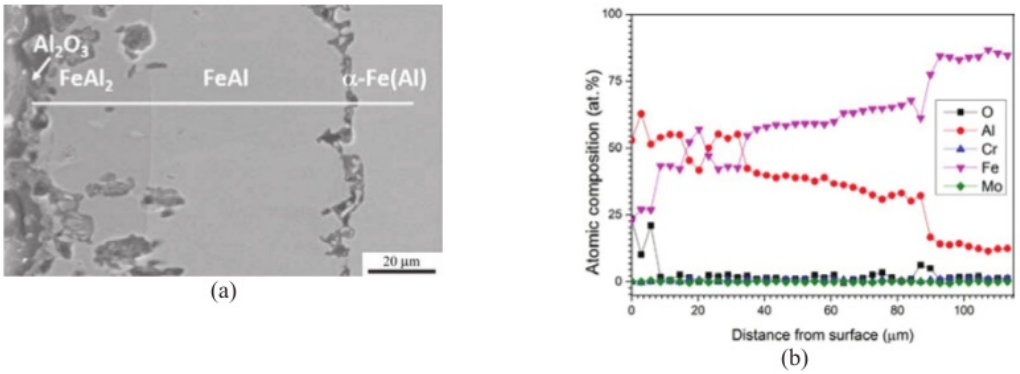

FIGURE 4. (a) SEM cross-sectional micrograph of Al-coated specimen oxidized at 850°C for 36 h and (b) its corresponding EDS line profiles of Fe, Al, Cr, O, and Mo

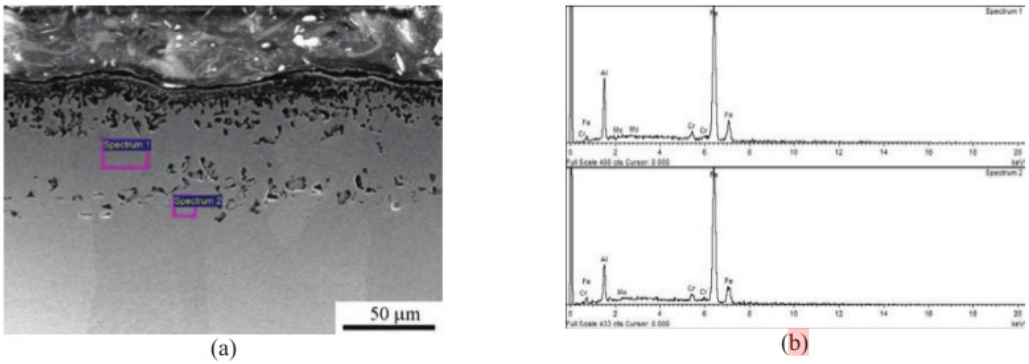

FIGURE 5. (a) SEM cross-sectional micrograph of the aluminide coating on AISI 4140 steel after isothermal oxidation at 850°C for 49 h and (b) EDS spectra for Fe, Al, Cr, and Mo

Cross-sectional SEM micrographs of aluminide steel (Fig. 5a) and EDS results (spectrum 1, Fig. 5b) from phase-constitution analysis reveal that the major phase in the aluminide layer as the oxidation time increased to 49 h was Fe_3Al with Al, Fe, Cr, and Mo compositions (at.%) of 25.10, 72.61, 2.05, and 0.23, respectively. EDS spectrum 2 (Fig. 5b) shows that the aluminide layer contains 18.91, 78.50, 2.32, and 0.27 at.%, Al, Fe, Cr, and Mo, respectively. These results show that longer oxidation time led to lower content of aluminum atoms of the aluminide layer on the steel substrate.

Figure 6 shows the surface SEM morphology of the oxide scales formed on the Al-coated specimen after air oxidation at 850°C for 49 h. There were two different structures of Al_2O_3 scales on the surface: α-Al_2O_3 with iron oxide nodules on the aluminide layer (Fig. 6a) and α-Al_2O_3 agglomerates on rod-shaped FeAl precipitates (Fig. 6b) formed in different areas. EDS analysis showed that the Cr and Fe content in the area of the agglomerates was 0.22 and 2.20 at.%, respectively. Those in the area of α-Al_2O_3 on the aluminide surface were 0.21 and 7.09 at.%, respectively. The surface morphology of the alumina scale is dense. Although iron oxide nodules also grew on the aluminide surface, the aluminide coating on the AISI 4130 steel underwent very slow oxidation. Agglomerates of the α-Al_2O_3 phase only grew on the rod-shaped FeAl precipitates after 49 h of oxidation. The rod-shaped FeAl phase resulted from the transformation of the $FeAl_2$ phase due to Al consumption. α-Al_2O_3 agglomerates grew relatively fast in the rod-shaped FeAl phase because of the high diffusivity of Al^{3+} during outward transport via screw dislocation [5]. In addition, the high Fe content (7.09 at.%) in the alumina scale might have contributed to the formation of iron oxide nodules via Al''' vacancy defects in the alumina layer [7].

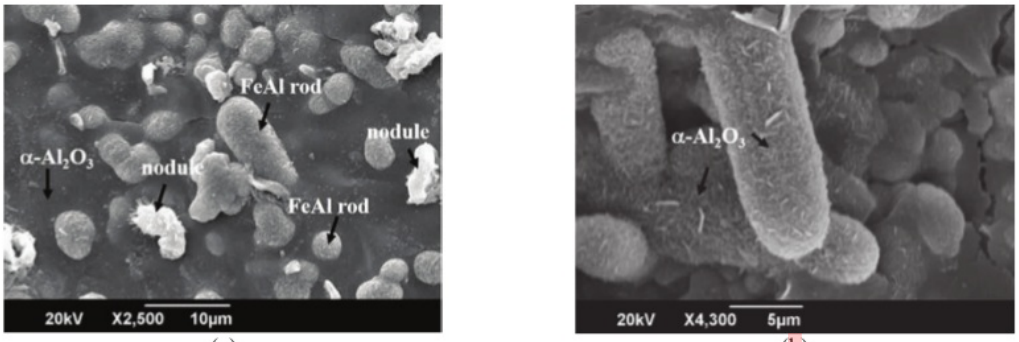

FIGURE 6. (a) SEM surface morphology of the Al-coated specimen and (b) α-Al_2O_3 agglomerates growing on the rod-shaped FeAl phases after isothermal oxidation at 850°C for 49 h

CONCLUSIONS

A hot-dipped aluminum coating has been applied to AISI 4130 steel to improve its oxidation resistance at 850°C. The oxidation kinetics follows a parabolic law, which is evident in the diffusion-controlled formation of the intermetallic phase consisting of Fe_2Al_5, $FeAl_2$, FeAl, and FeAl-Cr precipitates, as well as in the formation of the surface morphology of alumina scale. The aluminide coating provides good protection for the steel substrate by forming a protective alumina scale. The rate for the Al-coated steel is two to four orders of magnitude lower than that for bare steel. After oxidation at 850°C for 49 h, a fully dense and continuous alumina scale formed on the surface of the aluminide coating. Agglomerates of α-Al_2O_3 fine grains on the rod-shaped FeAl phase are attributed to the fast outward diffusion of Al atoms via screw dislocation.

ACKNOWLEDGMENT

The authors would like to thank to the Ministry of Research, Technology and Higher Education of the Indonesian Republic for funding support via the Grant Research of National Strategy under contract no. 153/UN26/8/LPPM/2015.

REFERENCES

1. R. K. S. Raman and A. Al-Mazrouee, Metall. Maters. Transactions A **38**, 1750–1759 (2007).
2. N. J. Simms and J. A. Little, Oxid. Metals **27**, 283–299 (1987).
3. R.V. Kumar, V. K. Tewari and S. Prakash, Metall. Maters Transactions A **38**, 54–57 (2007).
4. D. B. Lee, G. Y. Kim and J. G. Kim, Maters. Sci. Engineering A **339**, 109–116 (2003).
5. Y. Y. Chang, W. J. Cheng and C. J. Wang, Maters. Characterization **60**, 144–149 (2009).
6. C. J. Wang and S. M. Chen, Surf. Coat. Technology **200**, 6601–6606 (2006).
7. C. J. Wang and M. Badaruddin, Surf. Coat. Technology **205**, 1200–1205 (2010).
8. W. J. Cheng and C. J. Wang, Appl. Surf. Science **277**, 139– 145 (2013).
9. W. J. Cheng and C. J. Wang, Maters. Characterization **61**, 467–472 (2010).
10. Z. Zhan, Y. He, D. Wang and W. Gao, Oxid. Metals **68**, 243–251 (2007).

High-temperature oxidation behavior of aluminized AISI 4130 steel

ORIGINALITY REPORT

90%

SIMILARITY INDEX

PRIMARY SOURCES

1	aip.scitation.org Internet	2470 words — 80%
2	umexpert.um.edu.my Internet	150 words — 5%
3	intra.lipi.go.id Internet	47 words — 2%
4	www.repositorio.unicamp.br Internet	28 words — 1%
5	scienceline.mrl.ucsb.edu Internet	18 words — 1%
6	www.science.gov Internet	17 words — 1%
7	fisika.fmipa.unila.ac.id Internet	15 words — < 1%
8	repo-nkm.batan.go.id Internet	13 words — < 1%
9	science.sciencemag.org Internet	10 words — < 1%

EXCLUDE QUOTES ON EXCLUDE MATCHES OFF

EXCLUDE BIBLIOGRAPHY ON